

# Improved Extrapolation Methods of Data-driven Background Estimations in High Energy Physics

Suyong Choi and Hayoung Oh

Department of Physics, Korea University, Seoul 02841, Republic of Korea

E-mail: suyong@korea.ac.kr, hayoung.oh@cern.ch

**Abstract.** The data-driven methods of background estimations are widely used in order to obtain a more reliable description of backgrounds. In hadron collider experiments, data-driven techniques are used to estimate backgrounds due to multi-jet events, which are difficult to model correctly and are major sources of uncertainties. In this article, we propose an improvement on one of the most widely used data-driven methods used in the hadron collision environment, the “ABCD” method of extrapolation. We describe the mathematical background behind the data-driven methods and extend the idea to propose improvements to the methods. Through these methods, it is possible to significantly improve the prediction of backgrounds.

*Keywords:* Hadron collider, background estimation, multi-jet events

Submitted to: *J. Phys. G: Nucl. Part. Phys.*

## 1. Introduction

The Standard Model (SM) of particle physics is compatible with almost all of the measurements from particle experiments. In contrast to the successes on Earth, the astrophysical measurements seem to imply existence of energy component that cannot be explained by SM, and mount serious challenge.

Despite theoretical and experimental efforts, there is no direct evidence that any of the solutions proposed is correct. Moreover, it is not clear what direction should be taken in order to resolve the problem. Particles predicted by viable extensions of SM are already excluded beyond many TeV’s at the LHC [1]. It may turn out that these new states are massive enough to be beyond the reach of the LHC for direct production. The effect of these massive states will show up in the lower energy as a effective theory (EFT). Therefore, there is a trend towards EFT interpretations of the LHC results [2]. However, it does not exclude the possibility that interesting physics is waiting to be found in rarer and more complicated final states. For example, We may have to entertain the possibility of exotic final states [8, 9], where new states appear as a continuum rather than as a resonance, above backgrounds. In either case, better accuracy of background estimation is necessary.

For many processes of interest, automatic calculations to next-to-leading order (NLO) in strong interactions are accessible in modern Monte Carlo event generators [10]. However, even at the NLO, theoretical uncertainties are larger than statistical uncertainty for many processes at the LHC. And as the number of final-state hadronic jets increase, even the accuracy of NLO calculations decrease [11]. The parton showering, hadronization, and underlying events have smaller effect on the theoretical uncertainty, but nevertheless is not negligible.

To reduce the uncertainties related to background estimation, various data-driven estimation methods could be employed. Data-driven methods make use of the data in the “background” dominated region to estimate background contribution in the “signal” region, where interesting events may be found. The method of interpolating using side-bands is a canonical method. In analyses involving hadron collision data, we often employ a method of extrapolation, called “ABCD” data-driven background methods. It should be noted that data driven methods do not exclude the use of simulated data entirely. In this letter, We review the main idea behind data-driven methods and then extend on it to find an improvement to the extrapolation method.

## 2. Data-driven methods of background estimation

The concept of estimating backgrounds from the data itself is nothing new. Important discoveries in the history of particle physics would not have been possible without such estimations, given that the underlying theory of particle interactions were not very well known or had large uncertainties [3]-[7].

While there are many ways the data-driven methods can be divided, in this letter, we will group them into two categories. In the first category, there are data-driven methods that use interpolations from the measurements performed on the side bands. These methods are used when we look for a new particle state in a restricted range of kinematic phase space (usually mass). In the second category, there are methods we use when straight interpolations are difficult to employ. The methods that use extrapolations based on information in signal depleted region, fall in this group. The extrapolation methods, loosely called the “ABCD” method, are often used in hadron collider experiments, where predictions of multijet production processes have large uncertainties [12, 13]. For more complicated analyses, it could involve combinations of the two categories.

### 2.1. Interpolation methods

We briefly review the interpolation methods, which will give us ideas on how to extend and improve extrapolation methods. In an interpolation method, measurements are performed in the side-bands (or control regions) that surround the “signal” region and the information is combined to estimate the backgrounds in the signal region. In the absence of any other information, the minimal assumption is that the background would

have a smooth distribution.

Let us take a one dimensional example. We may assume that the signal region is in  $x_0 \sim x_0 + \Delta$ . Without loss of generality. The number of background in this region for a distribution of background described by  $f(x)$  may be expressed as  $F(x_0) \equiv \int_{x_0}^{x_0+\Delta} f(x)dx$ . Let us take a simple side-band of equal width to either side of the signal region. The backgrounds to the left(right) side band is  $F(x_0 - \Delta)$  ( $F(x_0 + \Delta)$ ), respectively. If we assume the series expansion is valid then we can express the entries in the side-bands as,

$$F(x_0 - \Delta) = F(x_0) - \Delta F'(x_0) + \Delta^2 \frac{1}{2} F''(x_0) - \Delta^3 \frac{1}{3!} F'''(x_0) + O(\Delta^4) \quad (1)$$

$$F(x_0 + \Delta) = F(x_0) + \Delta F'(x_0) + \Delta^2 \frac{1}{2} F''(x_0) + \Delta^3 \frac{1}{3!} F'''(x_0) + O(\Delta^4). \quad (2)$$

From the two side bands, the best estimate of  $F(x_0)$  is obtained by taking the average of the two:

$$F(x_0) = \frac{1}{2} [F(x_0 - \Delta) + F(x_0 + \Delta)] + O(\Delta^2), \quad (3)$$

which is a well-known result.

For a background, whose distribution is of the  $f(x) = ax + b$  form, the answer is exact. However, for a shape that has higher-order terms, this approximation may not be enough. If we allow two side-bands on each side, the terms proportional to  $\Delta^2$  can be eliminated.

$$F(x_0 - 2\Delta) = F(x_0) - 2\Delta F'(x_0) + 2\Delta^2 F''(x_0) - \Delta^3 \frac{8}{3!} F'''(x_0) + O(\Delta^4) \quad (4)$$

$$F(x_0 + 2\Delta) = F(x_0) + 2\Delta F'(x_0) + 2\Delta^2 F''(x_0) + \Delta^3 \frac{8}{3!} F'''(x_0) + O(\Delta^4) \quad (5)$$

The best estimate from two equal width side bands on each side is

$$F(x_0) = \frac{4}{6} [F(x_0 - \Delta) + F(x_0 + \Delta)] - \frac{1}{6} [F(x_0 - 2\Delta) + F(x_0 + 2\Delta)] + O(\Delta^4), \quad (6)$$

which is accurate for background distribution  $f(x)$  that is locally a cubic function. One can easily understand this since with one side band each side, we can fit a line through the two measurements points for interpolation, thus we can find the linear function exactly. And with two side bands on each side, we have four measurements, therefore, we can fit a cubic function for interpolation.

Usually, we deal with one-dimensional distribution that has sufficient number of events. Therefore, we can have many bins to gain information on the shape of the distribution. From this, we may be able to find an empirical function that best describes the differential distribution in the side bands.

If we extend to more than one dimension, it may not be obvious what function to use. Let us consider a rectangular signal region in  $x, y$  space between  $x_0 \sim x_0 + \Delta_x$  and  $y_0 \sim y_0 + \Delta_y$ . Altogether, we can use 8 side-bands, four on sides of the rectangle

and four regions on the corners. Without any prior knowledge on the background distributions, and using similar arguments as before, one can show that the best estimate for interpolation is given by

$$\begin{aligned}
F(x_0, y_0) \approx & \frac{1}{4} [2F(x_0 - \Delta_x, y_0) + 2F(x_0 + \Delta_x, y_0) \\
& + 2F(x_0, y_0 - \Delta_y) + 2F(x_0, y_0 + \Delta_y) \\
& - F(x_0 - \Delta_x, y_0 - \Delta_y) - F(x_0 + \Delta_x, y_0 - \Delta_y) \\
& - F(x_0 - \Delta_x, y_0 + \Delta_y) - F(x_0 + \Delta_x, y_0 + \Delta_y)] + O(\Delta^4) \quad (7)
\end{aligned}$$

## 2.2. "ABCD" extrapolation methods

We can use a different method of background estimation if the dependence of an observable on  $x$  and  $y$  are mostly factorizable, as:

$$F(x, y) = P_x(x)P_y(y) [1 + \epsilon(x, y)], \quad (8)$$

where we assume that the correlation is in the  $\epsilon$  function and is small  $|\epsilon| \ll 1$ . Then, the expected backgrounds in a rectangular region is mostly factorizable as well.

$$\begin{aligned}
F(x_0, x_1, y_0, y_1) &= \int_{y_0}^{y_1} \int_{x_0}^{x_1} P_x(x)P_y(y) [1 + \epsilon(x, y)] dx dy \\
&= \int_{x_0}^{x_1} P_x(x) dx \int_{y_0}^{y_1} P_y(y) dy \\
&\quad \times \left[ 1 + \frac{\int_{y_0}^{y_1} \int_{x_0}^{x_1} P_x(x)P_y(y)\epsilon(x, y) dx dy}{\int_{x_0}^{x_1} P_x(x) dx \int_{y_0}^{y_1} P_y(y) dy} \right] \\
&= S_x(x_0, x_1)S_y(y_0, y_1) [1 + \Sigma(x_0, x_1, y_0, y_1)], \quad (9)
\end{aligned}$$

where  $\Sigma$  is the average value of  $\epsilon$  over this range and depends on the amount of correlation between the two variables  $x$  and  $y$ . The  $S_x(S_y)$  is the integral of  $P_x(P_y)$  in range  $x_0 \sim x_1$  ( $y_0 \sim y_1$ ), respectively. For a fixed-width windows,  $x_1 = x_0 + \Delta_x$  and  $y_1 = y_0 + \Delta_y$ ,  $F$  is a function of  $x_0$  and  $y_0$ , so we can drop the arguments  $x_1$  and  $y_1$  as,

$$F(x, y) = S_x(x)S_y(y) [1 + \Sigma(x, y)]. \quad (10)$$

We can get an estimate of  $F(x, y)$  by taking suitable ratio of the  $F$ 's in the neighboring regions:

$$\begin{aligned}
& \frac{F(x - \Delta_x, y)F(x, y - \Delta_y)}{F(x - \Delta_x, y - \Delta_y)} \quad (11) \\
&= S_x(x)S_y(y) \left[ 1 + \Sigma(x, y) + \left( \frac{\partial \Sigma}{\partial x} \frac{\partial \Sigma}{\partial y} - \frac{\partial^2 \Sigma}{\partial x \partial y} \right) \Delta_x \Delta_y \right] + O(\Delta^3) \\
&= F(x, y) + O(\Delta^2),
\end{aligned}$$

where the  $\Delta$ 's stand for either  $\Delta_x$  or  $\Delta_y$ . The  $\Delta_x \Delta_y$  term would vanish if  $\epsilon(x, y)$  can be written as  $\epsilon(x, y) = \epsilon_x(x)\epsilon_y(y)$ , i.e, the distribution is completely factorizable. Therefore, the error of the estimation depends on the degree of correlation of  $x$  and  $y$ . In this derivation, we do not assume that  $S_x$  and  $S_y$  vary slowly, necessarily, but that  $\Sigma$  varies slowly enough that the series expansion is valid.

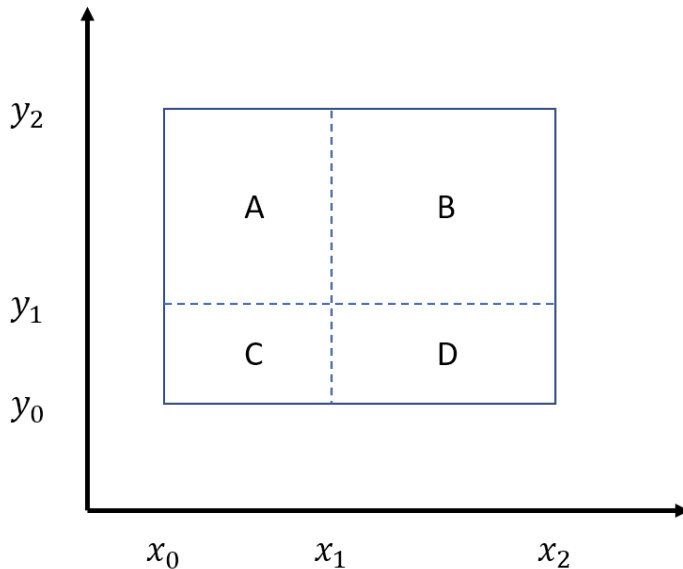


**Figure 1.** Four adjacent regions of the ABCD method.

This method is often referred to as the “ABCD” method (Eq. 11) or matrix method. In this method, two dimensional phase space is divided into four regions, one of which is the signal region and the neighboring three regions are the control regions. The choice of the two variables used for this purpose, depends on the physics case of interest, but should be uncorrelated as much as possible.

In hadron collision experiments, extrapolation methods are used to estimate the backgrounds due to strong interactions. Usually, signature of interest is expected at high energies or high particle multiplicities therefore, the interpolation methods cannot be used. The use of extrapolation is necessitated by the large uncertainty in prediction of multijet backgrounds.

The backgrounds are measured in signal-depleted region, usually in a lower energy and/or lower multiplicity region, and then, the information is extrapolated to the signal region. The information from the 3  $A$ ,  $B$ , and  $C$  control regions (or side bands), is used to estimate the backgrounds in the signal region,  $D$  (Fig. 1). Generally, we can express the estimate of  $F_D$  as  $\hat{F}_D$ ,

$$\begin{aligned}
 \hat{F}_D &= \frac{F_B}{F_A} \times F_C \\
 &= \frac{S_x(x_1, x_2) S_y(y_1, y_2) [1 + \Sigma(x_1, x_2, y_1, y_2)]}{S_x(x_0, x_1) S_y(y_1, y_2) [1 + \Sigma(x_0, x_1, y_1, y_2)]} \\
 &\quad \times S_x(x_0, x_1) S_y(y_0, y_1) [1 + \Sigma(x_0, x_1, y_0, y_1)] \\
 &= S_x(x_1, x_2) S_y(y_0, y_1) [1 + \Sigma(x_1, x_2, y_0, y_1)] + O(\Delta^2), \tag{12}
 \end{aligned}$$

where the  $\Delta$ 's are either  $x_1 - x_0$ ,  $x_2 - x_1$ ,  $y_1 - y_0$ , or  $y_2 - y_1$ .

The ABCD method cannot be used when one or both boundaries ( $x_2$  and/or  $y_2$ ) are taken to infinity, since  $\Delta \rightarrow \infty$ . In these cases, the ABCD method could still work if the distribution  $P_x(x)$  falls sharply as  $x$  increases. With this,  $\Sigma(x_1, x_2, y_0, y_1) \approx$

$\Sigma(x_1, x_1 + \delta_x, y_0, y_1)$ , remembering that the  $\Sigma$  is the average value of  $\epsilon$  in the given region, thus  $x_2$  is not as relevant since the data are distributed heavily towards lower values of  $x$ . Under these conditions, the Eq. 12 is still valid since,

$$\begin{aligned}
& \frac{1 + \Sigma(x_0, x_1, y_0, y_1)}{1 + \Sigma(x_0, x_1, y_1, y_2)} \times [1 + \Sigma(x_1, x_2, y_1, y_2)] \\
&= 1 + \Sigma(x_1, x_2, y_1, y_2) - \Delta_{y1}\Sigma_3(x_0, x_1, y_0, y_1) \\
&\quad - \Delta_{y2}\Sigma_4(x_0, x_1, y_0, y_1) + O(\Delta_y^2) \\
&\approx 1 + \Sigma(x_1, x_2, y_1, y_2) - \Delta_{y1}\Sigma_3(x_0, x_0 + \delta, y_0, y_1) \\
&\quad - \Delta_{y2}\Sigma_4(x_0, x_0 + \delta, y_0, y_1) + O(\Delta_y^2) \\
&\approx 1 + \Sigma(x_1, x_2, y_1, y_2) - \Delta_{y1}\Sigma_3(x_1, x_1 + \delta, y_0, y_1) \\
&\quad - \Delta_{y2}\Sigma_4(x_1, x_1 + \delta, y_0, y_1) + \Delta_{x1}\Delta_{y1}\Sigma_{31}(x_1, x_1 + \delta, y_0, y_1) \\
&\quad + \Delta_{x1}\Delta_{y2}\Sigma_{41}(x_1, x_1 + \delta, y_0, y_1) + O(\Delta_y^2) \\
&\approx 1 + \Sigma(x_1, x_2, y_0, y_1) + O(\Delta^2), \tag{13}
\end{aligned}$$

where  $\Sigma_i$  ( $\Sigma_{ij}$ ) is the partial derivative with respect to  $i$ th argument ( $i$  and  $j$  arguments), respectively, and  $\Delta$ 's are either  $\Delta_{x1}$ ,  $\Delta_{y1}$ , or  $\Delta_{y2}$ . In summary, in ABCD method, measurements in three regions neighboring the signal region can be used to give the accurate description to  $O(\Delta^2)$ , given that the correlation between the  $x$  and  $y$  are weak and the distribution is sharply falling in  $x$  and  $y$ .

### 3. Improving the data-driven extrapolation method

As was the case in interpolation, it is possible to improve the accuracy of extrapolation methods by including more control regions. We demonstrate the potential benefits with a simple example of multijet extrapolation in  $t\bar{t} + \text{multijets}$ .

#### 3.1. Extended ABCD method

Without loss of generality, we consider a problem of estimating the background in a hypothetical signal region  $x > x_0$  and  $y > y_0$  in Fig. 2. We assume that outside this region, the signal is a small fraction of the total.

Assuming again that the joint distribution in  $x$  and  $y$  are mostly factorizable, we can write the number of entries in the signal region as  $F(x_0, y_0) = S_x(x_0)S_y(y_0)[1 + \Sigma(x_0, y_0)]$ . By using the information in the region  $x_0 - \Delta_x \sim x_0$  as well as  $x_0 - 2\Delta_x \sim x_0 - \Delta_x$ , and similarly in the lower parts of signal region, one can show that the accuracy improves,

$$\begin{aligned}
F(x_0, y_0) &= \left[ \frac{F(x_0 - 2\Delta_x, y_0 - \Delta_y)F(x_0 - \Delta_x, y_0 - 2\Delta_y)}{F(x_0 - 2\Delta_x, y_0 - 2\Delta_y)} \right]^{\frac{4}{3}} \\
&\quad \times \left[ \frac{F(x_0 - \Delta_x, y_0)F(x_0, y_0 - \Delta_y)}{F(x_0 - \Delta_x, y_0 - \Delta_y)} \right]^{-\frac{1}{3}} + O(\Delta^3), \tag{14}
\end{aligned}$$

where  $\Delta$  stands for  $\Delta_x$  or  $\Delta_y$ . By combining information from more control regions in an optimal way, terms up to  $\Delta^2$  can be canceled exactly. In doing so, the effects of

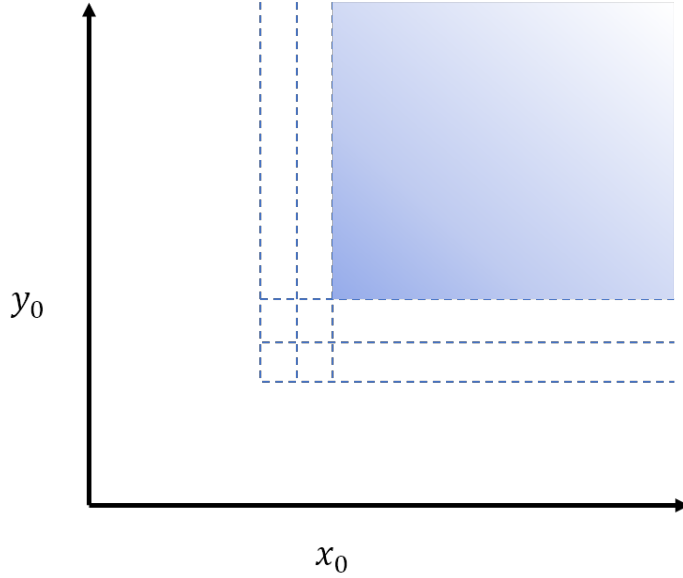


**Figure 2.** Regions in extended method. The upper right region is the signal region, while the rest are the control regions.

correlations among variables on the prediction are mitigated as well. In the appendix, we give an explicit expression for Eq. 14.

We can extend idea further by using information in eight control regions (Fig. 2), where it is possible to get accuracy of the  $O(\Delta^4)$  order:

$$\begin{aligned}
 F(x_0, y_0) &= \frac{F(x_0 - 2\Delta_x, y_0)F(x_0, y_0 - 2\Delta_y)}{F(x_0 - 2\Delta_x, y_0 - 2\Delta_y)} \\
 &\times \left[ \frac{F(x_0 - \Delta_x, y_0)F(x_0, y_0 - \Delta_y)}{F(x_0 - \Delta_x, y_0 - \Delta_y)} \right]^4 \\
 &\times \left[ \frac{F(x_0 - 2\Delta_x, y_0)F(x_0, y_0 - \Delta_y)}{F(x_0 - 2\Delta_x, y_0 - \Delta_y)} \right]^{-2} \\
 &\times \left[ \frac{F(x_0 - \Delta_x, y_0)F(x_0, y_0 - 2\Delta_y)}{F(x_0 - \Delta_x, y_0 - 2\Delta_y)} \right]^{-2} + O(\Delta^4). \quad (15)
 \end{aligned}$$

However, the feasibility of making use of many control regions depends on the statistics available. Since a control region with small statistics will obviously have larger statistical uncertainty. From practical considerations, it may be desirable to have fewer control regions. Here, we give an optimal expression for the case of five control regions, by allowing for two control region bins in either  $x$  or  $y$ , but not both. In the case of two control region bins in  $x$ , but one in  $y$ , the optimal combination of the control region measurements is

$$\begin{aligned}
 F(x_0, y_0) &= \left[ \frac{F(x_0 - \Delta_x, y_0)F(x_0, y_0 - \Delta_y)}{F(x_0 - \Delta_x, y_0 - \Delta_y)} \right]^2 \\
 &\times \left[ \frac{F(x_0 - 2\Delta_x, y_0 - \Delta_y)}{F(x_0 - 2\Delta_x, y_0)F(x_0, y_0 - \Delta_y)} \right] + O(\Delta_x^2 \Delta_y). \quad (16)
 \end{aligned}$$

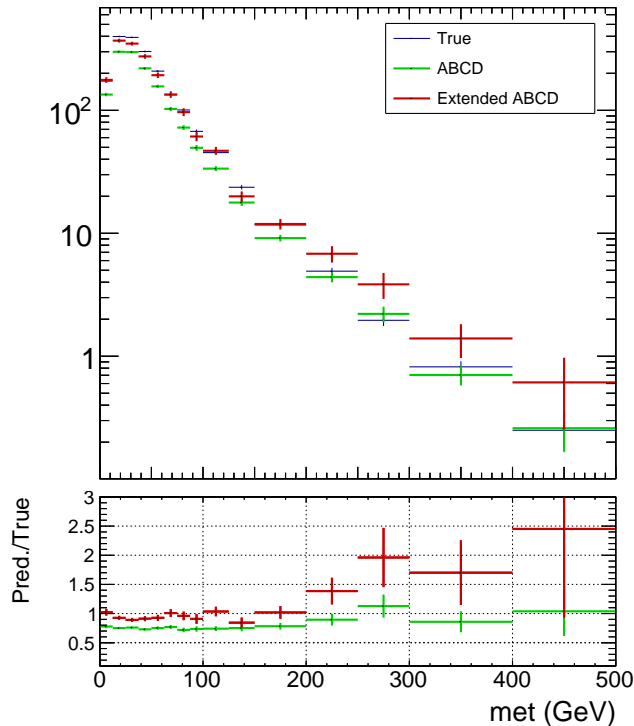


**Figure 3.** Missing transverse momentum distribution for  $N_j \geq 9$  and  $N_{b-jet} \geq 3$  using the standard ABCD method (green) and the extended ABCD method (red). The lower inset shows the ratio of the predictions to their true values. The error bars indicate the statistical uncertainties.

Again, the validity of the error depends on the weak correlation among the dependent variables  $x$  and  $y$ , as described by  $\epsilon(x, y)$ . We also assume that the  $\epsilon(x, y)$  varies slowly enough to allow for the series expansion.

### 3.2. Application of extended ABCD method to $t\bar{t}$ +multijets in hadronic channels

In this subsection, we apply the extended extrapolation method to  $t\bar{t}$ +multijets events and compare to the conventional ABCD method. The  $t\bar{t}$ +multijets processes are backgrounds to many of the searches for physics beyond the standard model. While calculation of  $t\bar{t} + jj$  are available at the next-to-leading order (NLO), it has relatively large theoretical uncertainties than desired [11]. Furthermore, the quoted uncertainties in the literature are on the overall inclusive cross sections, and in some phase space, the uncertainties on the the differential cross sections could be large. Improved accuracy to next-to-next-to-leading order calculations for these processes would be difficult to envision in the foreseeable future. Therefore, having a more reliable data-driven technique is important for these processes.

As an illustration of the improvement this method could bring, we apply the extended ABCD method to  $t\bar{t}+jj$  simulated sample. We generated one million events

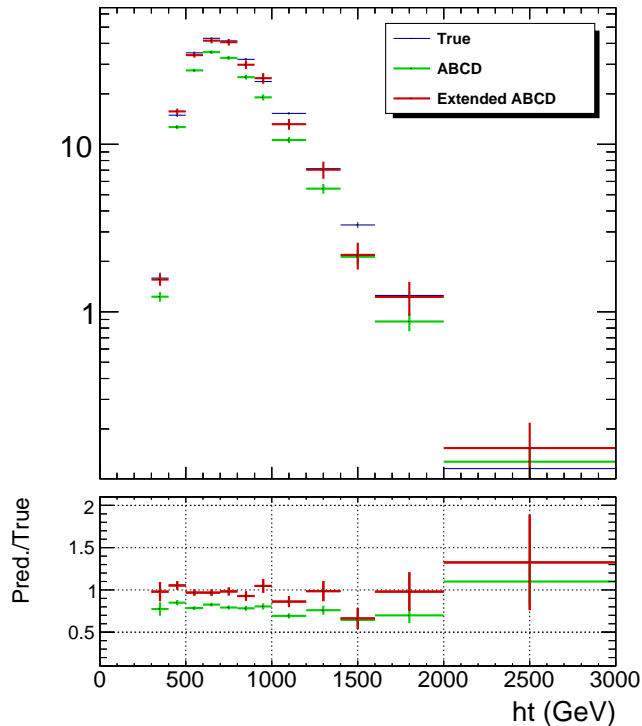


**Figure 4.** Distribution of  $H_T$  with hadronic jets for events  $N_j \geq 9$  and  $N_{b-jet} \geq 3$ , together with predictions from the standard ABCD method (green) and the extended ABCD method (red).

of  $pp \rightarrow t\bar{t}jj$  sample at  $\sqrt{s} = 14$  TeV with MG5aMC@NLO v2.61, to be used as a proxy for the real data. The extra partons are required to have  $p_T > 20$  GeV and  $|\eta| < 5.0$ . The events are hadronized with Pythia 8 and reconstructed with Delphes fast detector simulation and reconstruction in its default settings. For this example, we do not use NLO corrections. Also no matching procedure is applied.

In delphes, the reconstructed jets are required to be  $p_T > 30$  GeV and  $|\eta| < 2.4$ . We require zero isolated lepton that satisfies  $p_T > 20$  GeV and  $|\eta| < 2.4$  in an event. We apply Eq. 16, taking the number of hadronic jets as  $x$  and the number of  $b$ -tagged jets  $y$ . It could be applicable in a scenario where signature of interest consists of multijets and multiple  $b$ -tagged jets. The choice of variables depends on the problem of interest, but the method of extended ABCD would be generally applicable as long as the correlations are not too large.

For this example we take the signal region to be  $N_j \geq 9$  and  $N_{bjet} \geq 3$ . The control regions include  $N_j = 7, 8, \geq 9$  and  $N_{bjet} = 2, \geq 3$ , but excluding the signal region. Such a case can arise when large jet multiplicity region is of interest, such as, in the case of search for four top quark production in all hadronic channel.

Figure 3 shows missing transverse momentum distribution, comparing the estimations using the ABCD method and the extended ABCD method of extrapolation.

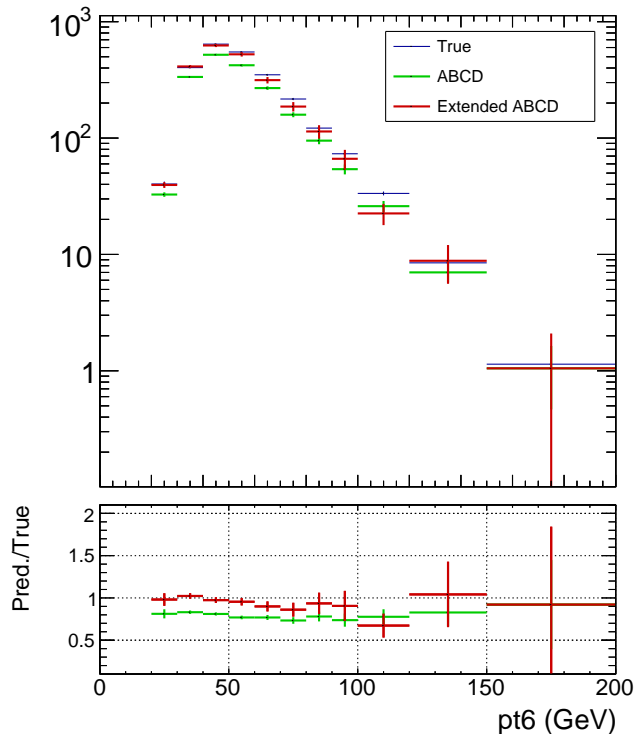


**Figure 5.** Distribution of transverse momentum  $p_T$  of the 6th leading hadronic jets for events  $N_j \geq 9$  and  $N_{b-jet} \geq 3$ , together with predictions from the standard ABCD method (green) and the extended ABCD method (red).

The overall normalization is predicted within 5%, while the ABCD method prediction is off by 18%. The extended ABCD method, however has larger statistical fluctuations due to the presence of more regions. We can also see a similar behavior in Fig. 4 where distribution of jet  $H_T$  is shown. In derivation of the extended ABCD method, the statistical uncertainty was not taken into account. In the limit of infinite statistics, the extended ABCD method would be closer to the truth. We can conclude that the decision to application of the extended method would depend on the statistics of the background available.

Figure 5 shows the distribution of the transverse momentum  $p_T$  of the sixth jet in an event. This figure illustrates limitations of the ABCD method in general when used in a purely data-driven mode. The sixth jet  $p_T$  distribution from  $N_j = 7, 8, \geq 9$  are used except those in the signal region. The lower multiplicity events do not have jet  $p_T$  reaching as far as those in the higher  $N_j$  events and the prediction is not able to reach the extreme high momentum. Therefore, in these cases, it would be desirable to use some smooth functions to fit the distributions to reduce the statistical fluctuations.

In these figures, we notice that the overall shape of the distributions are rather well described by the shape derived using the simple ABCD method, but the normalizations are off. Therefore, in this case, we could derive the normalization from the extended

ABCD method and apply it to the shape obtained with the ABCD method. However, it may be feature of this particular system that we are considering.

One might argue whether the extended ABCD method has any real benefits since, in many analyses, the normalizations are treated as nuisance parameters and constrained by fits to data. The extended ABCD method can provide smaller uncertainty on the prior of the normalization and could result in reduced background uncertainty in the end.

#### 4. Conclusion

In this letter, we outlined the mathematical bases for using data-driven extrapolation method of background estimation. We suggest an improvement to the ABCD method, by making use of more control regions. We give several generally applicable ways more control regions can be used. The extended ABCD method allows for a more accurate overall rate in prediction. Statistical uncertainty should be considered in deciding whether and how to apply the extended ABCD method. The differential distribution has less fluctuations with the ABCD method, but the overall normalization could still be predicted using the extended ABCD method.

#### Acknowledgments

This work was supported in part by the Korean National Research Foundation (NRF) mid-career grant NRF-2018R1A2B6005043.

#### Appendix A. Expressions for the extended ABCD methods

We give an explicit expression for Eq. 14 up to  $\Delta^3$ :

$$\begin{aligned}
S_x(x)S_y(y) & \left( 1 + \Sigma + \frac{2\Delta_x\Delta_y^2}{3(1+\Sigma)^2} \left( -2(\Sigma^{(0,1)})^2\Sigma^{(1,0)} + 2(1+\Sigma)\Sigma^{(0,1)}\Sigma^{(1,1)} \right. \right. \\
& \quad \left. \left. + (1+\Sigma) \left( \Sigma^{(0,2)}\Sigma^{(1,0)} - (1+\Sigma)\Sigma^{(1,2)} \right) \right) \right. \\
& \quad \left. + \frac{2\Delta_y\Delta_x^2}{3(1+\Sigma)^2} \left( -2(\Sigma^{(1,0)})^2\Sigma^{(0,1)} + 2(1+\Sigma)\Sigma^{(1,0)}\Sigma^{(1,1)} \right. \right. \\
& \quad \left. \left. + (1+\Sigma) \left( \Sigma^{(2,0)}\Sigma^{(0,1)} - (1+\Sigma)\Sigma^{(2,1)} \right) \right) \right) + O(\Delta^4) \quad (\text{A.1})
\end{aligned}$$

To reduce clutter, we omit the arguments  $(x, y)$  to  $\Sigma$  function. The superscripts  $(m, n)$  stand for partial derivatives, as  $\Sigma^{(m,n)} = \left(\frac{\partial}{\partial x}\right)^m \left(\frac{\partial}{\partial y}\right)^n \Sigma(x, y)$ .

And expression for Eq. 16 up to  $\Delta^3$  order is

$$\begin{aligned}
S_x(x)S_y(y) & \left( 1 + \Sigma + \frac{\Delta_x^2\Delta_y}{(1+\Sigma)^2} \left( \Sigma^{(0,1)} \left( (\Sigma+1)\Sigma^{(2,0)} - 2(\Sigma^{(1,0)})^2 \right) \right. \right. \\
& \quad \left. \left. + (1+\Sigma) \left( 2\Sigma^{(1,0)}\Sigma^{(1,1)} - (1+\Sigma)\Sigma^{(2,1)} \right) \right) \right) + O(\Delta^4) \quad (\text{A.2})
\end{aligned}$$

## References

- [1] D. del Re, *Exotics at the LHC*, PoS (ICHEP2018) 710.
- [2] A. Grohsjean, *EFT interpretations across LHC experiments and efforts towards global analyses*, DESY PUBDB-2019-02044, doi:10.3204/PUBDB-2019-02044.
- [3] J. J. Aubert, et al., *Experimental Observation of a Heavy Particle J*, Phys. Rev. Lett. **33** (1974) 1404.
- [4] J. Augustin, et al., *Discovery of a Narrow Resonance in  $e^+e^-$  Annihilation*, Phys. Rev. Lett. **33** (1974) 1406.
- [5] S. W. Herb, et al., *Observation of a Dimuon Resonance at 9.5 GeV in 400-GeV Proton-Nucleus Collisions*, Phys. Rev. Lett. **39** (1977) 252.
- [6] F. Abe, et al. (CDF Collaboration). *Observation of Top Quark Production in  $p\bar{p}$  Collisions with the Collider Detector at Fermilab*, Phys. Rev. Lett. **74** (1995) 2626.
- [7] S. Abachi, et al. (DØ Collaboration). *Observation of the Top Quark*, Phys. Rev. Lett. **74** (1995) 2632.
- [8] H. Cai, et al., *SUSY Hidden in the Continuum*, Phys. Rev. D **85** (2012) 015019.
- [9] C. Gao, et al., *Collider Phenomenology of a Gluino Continuum*, arXiv:1909.04061 [hep-ph].
- [10] J. Alwall et al., *The automated computation of tree-level and next-to-leading order differential cross sections, and their matching to parton shower simulations*, J. High Energ. Phys. (2014) 2014: 79.
- [11] G. Bevilacqua, M. Worek, *On the ratio of  $t\bar{t}b\bar{b}$  and  $t\bar{t}j\bar{j}$  cross sections at the CERN Large Hadron Collider*, J. High Energ. Phys. (2014) 2014: 135.
- [12] S. Abachi et al. (DØ Collaboration), *Search for the top quark in  $p\bar{p}$  collisions at  $\sqrt{s} = 1.8$  TeV*, Phys. Rev. Lett. **72** (1994) 2138.
- [13] S. Abachi et al. (DØ Collaboration), *Search for High Mass Top Quark Production in  $p\bar{p}$  collisions at  $\sqrt{s} = 1.8$  TeV*, Phys. Rev. Lett. **74** (1995) 2422.
- [14] O. Behnke et al., *Data Analysis in High Energy Physics*, Wiley-VCH Verlag GmbH & Co. KGaA, (2013) pg. 348.